# Probabilistic Model for Polycrystalline Microstructures with Application to Intergranular Fracture

Sanjay R. Arwade, A.M.ASCE,[1] and Mircea Grigoriu, F.ASCE[2]

**Abstract:** A two part probabilistic model for polycrystalline microstructures is described. The model utilizes a Poisson–Voronoi tessellation for the grain geometry and a vector random field model for the crystallographic orientation. The grain geometry model is calibrated to experimental data through the intensity of the Poisson point field underlying the Poisson–Voronoi tessellation and the orientation random field is calibrated to experimental data through its marginal distributions and second moment properties. Realizations of the random microstructure are generated by use of translation methods and are used, with simplified mechanical models, to investigate the problem of intergranular fracture. It is found that intergranular cracks exhibit some statistical properties of a scaled Brownian motion process.

**DOI:** 10.1061/(ASCE)0733-9399(2004)130:9(997)

**CE Database subject headings:** Microstructures; Fracture mechanics; Monte Carlo method; Probabilistic methods.

## Introduction

The goals of this paper are to (1) develop a probabilistic model for the microstructure of polycrystalline materials, and (2) use Monte Carlo simulation methods to determine statistics of intergranular cracks in synthetic microstructures. The fracture mechanics problem considered is that of quantifying the uncertainty in the trajectory of an intergranular crack in a random heterogeneous microstructure.

A significant body of research exists which addresses the modeling of random polycrystalline microstructures and their attendant material properties. In several studies a deterministic grain geometry is used—a tessellation of space filling truncated octahedra—while random material properties are assigned to the grain boundaries (Anderson and Rice 1985; Wilkinson 1988; Harlow et al. 1996). Random two-dimensional grain geometries have been generated by either perturbation of a deterministic grain geometry (van der Giessen and Tvergaard 1994a,b), or use of random tessellations (Ballarini et al. 1999). Iterative methods have been proposed for introducing the spatial correlation of material properties to random polycrystals (Gertsman et al. 1992, 1996; Gertsman 1997). It has not yet been established, however, whether these methods can match experimental data. A recent success has been achieved in the simulation of polycrystalline microstructures with the development of a method for automatic finite element meshing of random two-dimensional grain geometries (Weyer et al. 2002).

[1]Assistant Professor, Dept. of Civil Engineering, Johns Hopkins Univ., 3400 N. Charles St., Baltimore, MD 21218. E-mail: srarwade@jhu.edu

[2]Professor, Dept. of Civil and Environmental Engineering, Cornell Univ., Ithaca, NY 14853. E-mail: mdg12@cornell.edu

Note. Associate Editor: Gerhart I. Schueller. Discussion open until February 1, 2005. Separate discussions must be submitted for individual papers. To extend the closing date by one month, a written request must be filed with the ASCE Managing Editor. The manuscript for this paper was submitted for review and possible publication on June 24, 2003; approved on February 24, 2004. This paper is part of the ***Journal of Engineering Mechanics***, Vol. 130, No. 9, September 1, 2004. ©ASCE, ISSN 0733-9399/2004/9-997–1005/$18.00.

The primary contribution of this paper is the introduction of a random field model for the material properties—through the crystallographic orientation—which is capable of matching spatial correlation which may exist in real materials. This random field is conditional on the random grain geometry, thereby providing a physically realistic coupling between the random material properties and random grain geometry.

The work is motivated by the observation that the proportion of the service lifetime of a structural component in which macroscopic damage is present is small. For a significant portion of the lifetime of a structural component the length scale of the damage processes acting in the material is small compared to the length scale of the microstructure. An example is a crack with a length which is of the same order of magnitude as the average grain diameter. To reliably predict, therefore, the service lifetime of a structural component, it is important to be able to predict the rates of initiation and growth of small scale damage in microstructured materials. Any such predictions must include a quantification of the uncertainty inherent to the problem. This uncertainty originates both from uncertainty in loads and in features of the material microstructure.

This work represents a first step towards that goal in introducing a framework for numerical simulation of random polycrystalline materials. Fig. 1 shows the organization of the framework. Material data are used to develop probabilistic models, and samples generated from these models are used in the simulation of crack propagation. The results of these simulations constitute simulated data regarding the material state and can in turn be used to develop probabilistic models for the evolved material.

The paper is divided into two main parts. Probabilistic modeling of the material microstructure is presented first. Statistics of experimental data gathered from the literature are used to calibrate probabilistic models for two features of the polycrystalline microstructure, the grain geometry and the crystallographic orientation, both modeled in two dimensions. A method is then presented for efficiently generating realizations of these polycrystalline microstructures. In the second part of the paper an example application is presented. Monte Carlo simulation on realizations generated from the probabilistic material models is used to quan-

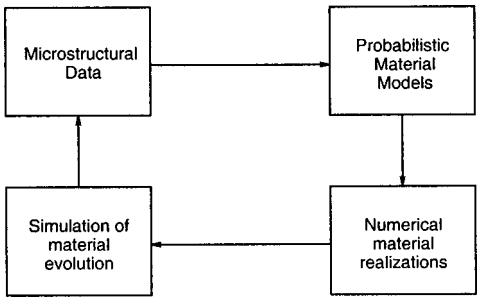


**Fig. 1.** Flow chart showing framework for probabilistic modeling and simulation of polycrystalline material evolution

tify the uncertainty in the trajectory of an intergranular crack in a random polycrystalline material. The crack trajectory is computed based on a simplified fracture mechanics model which considers the interaction between the random grain geometry and the random material properties resulting from the crystallographic orientation.

## Microstructural Measurements

### *Definitions*

Two features of the material microstructure are addressed in this paper, the grain geometry and crystallographic orientation. Measurements of these features have been provided by other researchers or gathered from the literature. Before proceeding to a discussion of the data, a brief definition of crystallographic orientation is now given.

The atoms of crystalline solids are arranged periodically on a three-dimensional lattice. This lattice can take several geometric forms, including the simple cubic lattice, the face- and body-centered cubic lattices, and the hexagonal lattice. In each case the periodic nature of the lattice provides a convenient definition of the crystal coordinate system (Fig. 2). While the crystal lattice defines the crystal coordinate system, a reference coordinate system can be defined relative to some laboratory or component frame of reference. The orientation is the transformation from the reference coordinate system to the crystal coordinate system. The orientation, a three-dimensional rotation, can be represented in a variety of mathematical forms [see Randle (1993) and Kumar and Dawson (1998) for in depth discussions of the various representations]. Here two representations are used. The Euler angle representation (Bunge 1982) and the axis/angle representation (Randle 1993).

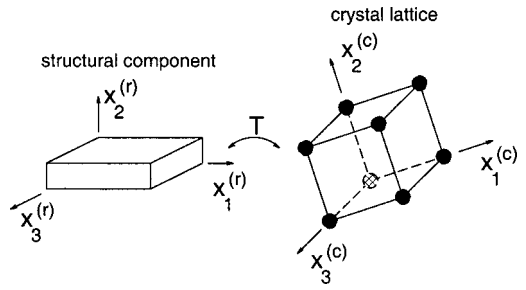


**Fig. 2.** Schematic illustration of crystalline lattice structure showing a possible definition of the crystal coordinate system along with a reference coordinate system defined relative to the geometry of a structural component. The rotation *T* maps the reference coordinates onto the crystal coordinates.

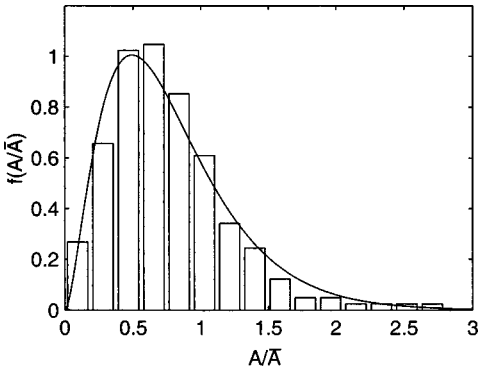


**Fig. 3.** Distribution of grain sizes in aluminum thin foil sample. Best fit gamma distribution is also shown. Reproduced from data given by Fradkov et al. (1985).

In the Euler angle representation the orientation is given by three angles which describe the three-dimensional rotation from the reference to crystal coordinate system. These three angles are typically denoted $[\phi_1,\Phi,\phi_2]$. Here an alternative notation is introduced in which $\psi_1=\phi_1$, $\psi_2=\Phi$, and $\psi_3=\phi_2$. This notation is introduced so that the Euler angles can be conveniently expressed as the vector $\boldsymbol{\psi}=[\psi_1,\psi_2,\psi_3]^T$. In the axis/angle representation the orientation is given by a single angle of rotation $\theta$ which is applied about an axis in $\mathbb{R}^3$. The axis/angle representation is particularly useful since the angle $\theta$ can be used as an approximate scalar representation of orientation.

While orientation describes the rotation from a reference coordinate system to a crystal coordinate system, misorientation describes the rotation from one crystal coordinate system to another. The misorientation, therefore, characterizes the difference in orientation between two crystal lattices. The axis/angle representation of misorientation is particularly useful since it provides, in the form of the angle $\theta$, a scalar quantification of the difference between two orientations. If the axis/angle representation of the misorientation between two lattices has a large angular component $\theta$ then the lattices can be said to be highly misoriented. It is useful to be able to make such statements when examining the strength of grain boundaries, which are discontinuities in the lattice orientation. The misorientation angle between grains *i* and *j* is denoted $\theta_{ij}$.

A complete characterization of grain geometry requires quantification of two parameters, the grain size and the grain shape. Quantification of grain shape remains an unsolved problem, with most existing techniques consisting of calculation of the aspect ratios of the grains. Grain size, on the other hand, can be quite easily quantified. Three methods are commonly used, corresponding to whether one-, two-, or three-dimensional measurements are desired. The line intercept method provides measurements of grain diameters, direct measurement of grain cross sectional areas is possible, and serial sectioning can provide approximate but direct measurement of grain volumes (Okazaki and Conrad 1972; Rhines and Patterson 1982; Fradkov et al. 1985). It has been shown that the average grain diameter, area, and volume are proportionally related so that measurement of one represents a complete characterization of the grain size (Okazaki and Conrad 1972).

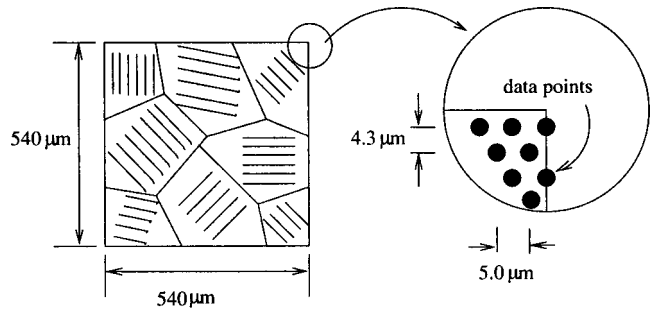


**Fig. 4.** Schematic illustration of layout of orientation measurements on materials surface. The sets of parallel lines are meant to indicate the local crystallographic orientation.

### *Experimental Data and Statistics*

For polycrystalline materials the grain size, as measured in one, two, or three-dimensions, has been found to be well approximated by a gamma random variable. The gamma random variable is defined by the probability density function (pdf)

$$f(x,\alpha_1,\alpha_2)=\frac{x^{\alpha_1-1}e^{-x/\alpha_2}}{\alpha_2^{\alpha_1}\Gamma(\alpha_1)} \tag{1}$$

where $\Gamma(\cdot)$ is the gamma function; and $\alpha_1$ and $\alpha_2$ are parameters of the distribution.

Fradkov et al. (1985) give the results of experimental measurements of the grain area of the crystals of a sample of thin aluminum foil. The data are reproduced in Fig. 3 in the form of a histogram of the normalized grain area $A/\bar{A}$. The histogram is overlaid with the best fit gamma pdf which has parameters $\alpha_1=2.79$ and $\alpha_2=0.29$.

It has recently become possible to obtain measurements of the local crystallographic orientation with very high resolution using the method of electron backscatter diffraction (EBSD) (Adams 1993; Adams et al. 1994). Using EBSD it is possible to measure the crystallographic orientation at the surface of a crystalline material with a resolution of 1 to 2 μm. The data obtained for the current analysis consist of 14,016 measurements taken on a regular grid over a 540 μm×540 μm region of 2000 series aluminum alloy (D. Mika, personal communication, 1997) (see Fig. 4 for a schematic of the measurement layout). The sample region contains cross sections of approximately 120 grains.

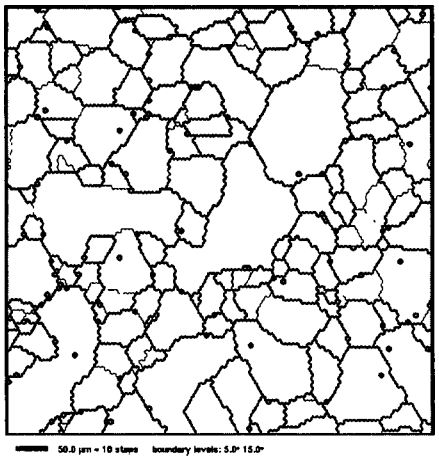

**Fig. 5.** Grain geometry of material sample as determined by misorientation calculation. Grain boundaries determined with cutoff misorientation angle of $\theta=15°$ (figure courtesy D. P. Mika).

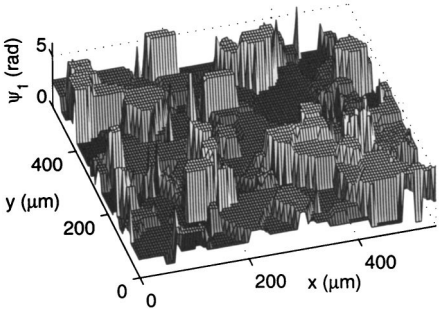


**Fig. 6.** Surface plot of Euler angle $\psi_1$

Fig. 5 shows the grain geometry of the sample. The lines, representing the grain boundaries, are found by considering the misorientation between the lattices at adjacent measurement points. If the misorientation angle θ from the axis/angle representation of the misorientation is found to be greater than 15° then a grain boundary is assumed to exist between the measurement points. From this representation of the grain geometry one can observe that the grain structure appears quite regular with the exception of a few large, irregularly shaped grains.

Fig. 6 shows $\psi_1$, the first Euler angle, plotted as a surface. Data are taken from the same experimental set as described above. The surface plot of the data shows the randomness of the crystallographic orientation, as well as the fact that the orientation is nearly constant within individual grains, and has discontinuities at the grain boundaries.

Some statistics of the orientation data are now given. Marginal pdfs of the three Euler angles are estimated, as are spatial auto- and cross-correlation functions for the three Euler angles. These statistics will be used in the next section to motivate a probabilistic model for the orientation.

Histograms of the Euler angles are shown in Fig. 7, with the corresponding cumulative distribution functions in Fig. 8. The statistics up to fourth order are given in Table 1. The histograms and statistics show that the random Euler angles are highly non-Gaussian. The histograms can be compared qualitatively to the Gaussian pdf, and the skewness ($\gamma_3$) and kurtosis ($\gamma_4$) can be compared to the values for the Gaussian distribution, $\gamma_3=0$ and $\gamma_4=3$. Any probabilistic model of the orientation must therefore be able to reproduce the non-Gaussianity of the data.

It is assumed throughout that the orientation field

1. Is weakly stationary (spatially homogeneous) and isotropic, and

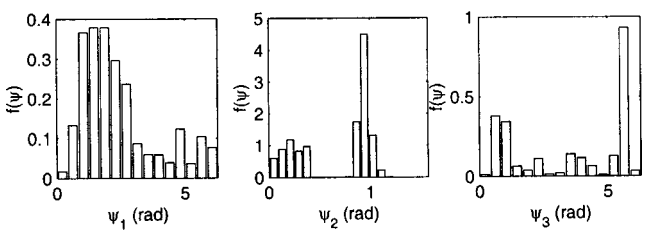


**Fig. 7.** Histograms of Euler angles showing highly non-Gaussian nature of the data

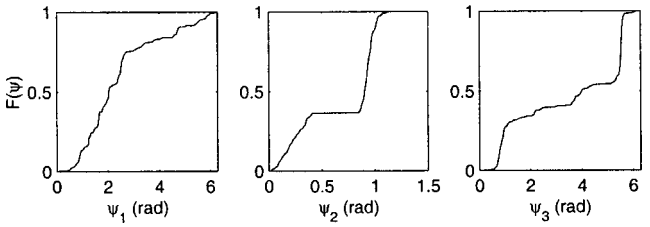


**Fig. 8.** Cumulative distribution functions of Euler angles as estimated from experimental data

2. Has marginal distributions which are invariant under translations.

These assumptions allow a simple estimation of the spatial correlation functions of the orientation.

Let $\mathbf{z}_j$, $j=1,\ldots,n$, be the points in a coordinate system labeled $(x_1,x_2)$, at which measurements were taken. In the current example $n=14{,}016$. The three Euler angles at these measurement points $\mathbf{z}_j$ are then denoted by $\psi_i(\mathbf{z}_j)$, $i=1,2,3$. Let also $\psi_i^{(1)}(\mathbf{z}_j,d)$ be the value of $\psi_i$ at $\mathbf{z}_j+d\mathbf{e}_1$ and $\psi_i^{(2)}(\mathbf{z}_j,d)$ be the value of $\psi_i$ at $\mathbf{z}_j+d\mathbf{e}_2$, where $\mathbf{e}_i$ is a unit vector in the $x_i$ direction and $d$ is a scalar separation distance. The auto- and cross-covariance functions are defined by

$$c_{pq}(d)=E[(\psi_p(\mathbf{y})-\mu_p)(\psi_q(\mathbf{y}+d\mathbf{n})-\mu_q)] \tag{2}$$

where $\mathbf{y}$ is an arbitrary position in the domain of the polycrystal and $\mathbf{n}$ is an arbitrarily oriented unit vector. Using the notation described above, estimates of these functions can be obtained by

$$\hat{c}_{pq}(d)\approx\frac{1}{2m}\sum_{j=1}^{m}\sum_{k=1}^{2}[\psi_p(\mathbf{z}_j)-\mu_p][\psi_q^{(k)}(\mathbf{z}_j,d)-\mu_q] \tag{3}$$

where $m$ is the number of points $\mathbf{z}_i$ for which $\mathbf{z}_i+d\mathbf{e}_1$ and $\mathbf{z}_i+d\mathbf{e}_2$ remain in the domain of measurement. As $d$ increases, so $m$ decreases.

From the estimated correlation functions estimates of the normalized covariance functions can be obtained by

$$\hat{\rho}_{pq}(d)=\frac{\hat{c}_{pq}(d)}{\sqrt{\hat{c}_{pp}(0)\hat{c}_{qq}(0)}} \tag{4}$$

Normalized covariance functions estimated from the data set described above are shown in Fig. 9. Best fit exponential decay functions $a\exp(-bd)$ computed for the normalized covariance functions have the parameters given in Table 2. Also shown in the table are the computed values of the correlation lengths $d_{c,ij}$. The correlation length is here defined such that

$$d_{c,ij}=\min\{d:\ \rho_{ij}(d)<e^{-1}\} \tag{5}$$

That is, the correlation length is the separation distance at which the scaled covariance first takes values less than $e^{-1}$.

To provide a physical interpretation of the correlation lengths, recall that the sample from which data were collected has dimension 540 μm×540 μm, or area 291,600 $\mu m^2$. With approximately 120 grains in the sample, the average grain radius is approximately 27 μm. The estimated correlation distances reveal that for this particular material sample the correlation between the orientation in neighboring grains is very small. Other investigators have, however, found long range correlations in orientations in various aluminum alloy polycrystals (Adams et al. 1994). For this reason, the probabilistic model presented in the next section allows for the possibility of orientation correlation between grains despite the evidence against such correlations in the current data set.

**Table 1.** Statistics of Euler Angles

| | Mean (μ) | Standard deviation (σ) | Skewness ($\gamma_3$) | Kurtosis ($\gamma_4$) |
|---|---|---|---|---|
| $\psi_1$ | 2.43 | 1.45 | 1.04 | 3.20 |
| $\psi_2$ | 0.683 | 0.358 | −0.616 | 1.58 |
| $\psi_3$ | 3.52 | 2.08 | −0.296 | 1.31 |

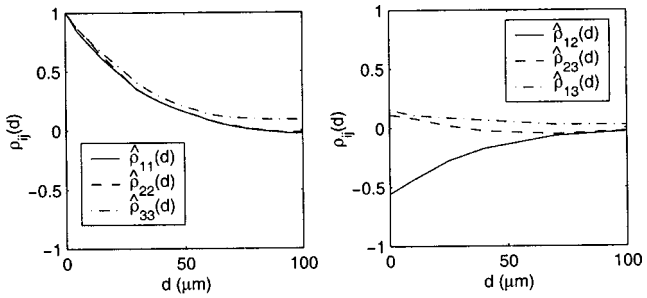


**Fig. 9.** Auto- and cross-correlation functions of Euler angles. Estimated based upon assumption of stationarity and isotropy.

## Probabilistic Models

A probabilistic model for polycrystalline microstructures is now presented. First, the Voronoi tessellation is proposed as a model for the grain geometry of polycrystalline materials. Second, a random field model is developed for the crystallographic orientation. Finally, a procedure for generating realizations of the random microstructure is given.

### *Grain Geometry*

The Voronoi tessellation has been used as a model for a variety of material microstructures, including the grain geometry of polycrystals. Here the Voronoi tessellation is implemented as a model for the two-dimensional grain geometry of the aluminum polycrystal under examination.

Given a domain $D\subset\mathbb{R}^2$ with $n$ nucleation points $\mathbf{c}_i\in D$, $i=1,\ldots,n$, the Voronoi tessellation divides $D$ into $n$ polygons, or cells, defined by

$$P_i=\{\mathbf{x}\in D|\|\mathbf{x}-\mathbf{c}_i\|<\|\mathbf{x}-\mathbf{c}_j\|,j\neq i\} \tag{6}$$

The geometric interpretation of this definition is that the cell $P_i$ contains all points in $D$ which are closer to the nucleus $\mathbf{c}_i$ than any other nucleus. The region $B$ defined by $B=\{\mathbf{x}:\ \mathbf{x}\notin P_i\}$, $i$

**Table 2.** Parameters of Orientation Scaled Covariance Functions as Estimated from Data

| | $a_{ij}$ | $b_{ij}$ | $d_{c,ij}$ (μm) |
|---|---|---|---|
| $\rho_{11}(d)$ | 1.0 | 0.036 | 27 |
| $\rho_{22}(d)$ | 1.0 | 0.035 | 28 |
| $\rho_{33}(d)$ | 1.0 | 0.030 | 33 |
| $\rho_{12}(d)$ | −0.57 | 0.030 | 14 |
| $\rho_{13}(d)$ | 0.14 | 0.021 | – |
| $\rho_{23}(d)$ | 0.13 | 0.012 | – |

Note: No entry indicates that the maximum value of $Pij^{(d)}$ is less then $e^{-1}$.

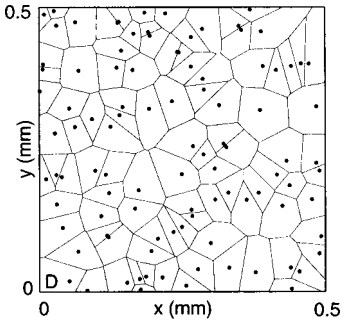


**Fig. 10.** Example Poisson–Voronoi tessellation with 100 grains and spatially invariant intensity

$=1,\ldots,n$, has zero area and defines the network of cell, or grain, boundaries. The polygons defined by the tessellation have straight edges and are convex. Use of the Voronoi tessellation as a model for grain geometry implies the physical assumptions that grain growth initiates simultaneously at all nuclei and that grain growth is stationary and isotropic.

Modeling of the nucleation points of the tessellation by a Poisson point field allows calibration of the average grain area to experimental measurements and introduces uncertainty into the grain geometry. A stationary Poisson point field is chosen since the experimental measurements show no evidence of spatially varying average grain size. The characteristics of a stationary Poisson point field are determined completely by the intensity of the field, denoted by $\lambda$. The average number of grains in any sample is a Poisson random variable with mean $\lambda A$, where $A$ is the area of the sample. Since the material sample has 120 grains in an area of 540 $\mu$m$\times$540 $\mu$m, the intensity is calculated to be

$$\lambda = \frac{120 \text{ grains}}{(0.540 \text{ mm})^2} = 412 \text{ grains/mm}^2 \tag{7}$$

A sample of the random grain geometry produced by the two part model of a Poisson point field for the grain nuclei and a Voronoi tessellation for the grains themselves is shown in Fig. 10. The sample domain is $D=[0,0.5]^2$ mm and the number of grains in this sample is 100. Comparison with Fig. 5 shows a qualitative similarity in the grain geometry although the Voronoi tessellation is not able to reproduce the anomalously large, concave grains seen in the actual material sample.

### Crystallographic Orientation

The spatial variability of the crystallographic orientation suggests a random field as an appropriate probabilistic model. A vector random field which is stationary in its marginal distributions and second moment properties can be calibrated to the statistics estimated for the experimental data. The vector random field is then

$$\boldsymbol{\Psi}(\mathbf{x}) = \begin{bmatrix} \Psi_1(\mathbf{x}) \\ \Psi_2(\mathbf{x}) \\ \Psi_3(\mathbf{x}) \end{bmatrix} \tag{8}$$

with marginal cumulative distribution functions shown in Fig. 8 and denoted by $F_i(\psi)$ $i=1,2,3$. The spatial variation of the orientation field is characterized in second moment by the matrix covariance function $\mathbf{c}(d)$ or the normalized matrix covariance function $\boldsymbol{\rho}(d)$. The component normalized covariance functions $\rho_{ij}(d)$ are set equal to the best fit exponential decay functions of Table 2.

Non-Gaussianity of the orientation is accommodated by letting the orientation field $\boldsymbol{\Psi}(\mathbf{x})$ take the form of a translation field (Grigoriu 1995). A translation field is a non-Gaussian random field which is a memoryless transformation of a Gaussian random field, called the Gaussian image of the translation field. For the orientation field this transformation is given by

$$\Psi_i(\mathbf{x}) = F_i^{-1}\{\Phi[V_i(\mathbf{x})]\} = g_i[V_i(\mathbf{x})] \tag{9}$$

where $F_i^{-1}(\cdot)$ is the inverse cdf of Euler angle $\psi_i$; $\Phi(\cdot)$ is the standard Gaussian cdf; and $V_i(\mathbf{x})$ is component $i$ of a Gaussian random vector field which has mean zero, unit variance, and a matrix of normalized covariance functions $\boldsymbol{\xi}(d)$ which are defined by

$$\mu_i\mu_j + \sigma_i\sigma_j\rho_{ij}(d) = \int_{-\infty}^{\infty}\int_{-\infty}^{\infty} g_i(y_1)g_j(y_2)\phi[y_1,y_2;\xi_{ij}(d)]dy_1dy_2 \tag{10}$$

where $\xi(\cdot,\cdot;\rho)$ is the bivariate standard normal density function with correlation coefficient $\xi$. The integral of Eq. (10) is typically calculated by numerical integration. The scaled covariance matrix $\boldsymbol{\xi}(d)$ of the Gaussian image $\mathbf{V}(\mathbf{x})$ of $\boldsymbol{\Psi}(\mathbf{x})$ must usually be calculated iteratively since Eq. (10) gives $\boldsymbol{\rho}$ in terms of $\boldsymbol{\xi}$.

Simulation of random polycrystalline microstructures is accomplished by first generating a realization of the random grain geometry and then generating a realization of the orientation field conditional upon the sample grain geometry. This procedure is now described for a two-dimensional domain $D$.

Generation of the sample grain geometry is straightforward, and consists of the following steps:

1. Generate a realization $n$ of the Poisson random variable $N$ with mean $\bar{N}=\lambda\int_D dA$.
2. Generate $n$ independent points $\mathbf{c}_i$, $i=1,\ldots,n$ uniformly distributed in $D$. These points serve as the grain nuclei.
3. Calculate the Voronoi tessellation associated with the nuclei $\mathbf{c}_i$ using existing algorithms such as the *qhull* algorithm implemented in *MATLAB*.

Generation of a realization of the orientation field, a vector random field, is complicated by the fact that the orientation field is characterized by discontinuities at the grain boundaries. Since no currently available simulation methods are able to produce such samples, a scheme is introduced which takes advantage of the already created grain geometry sample. This approach assumes that the orientation is constant within each grain. This assumption reduces the problem of simulation of the orientation field to the generation of a sample of a vector of orientations, one for each grain.

The $n$ orientations are generated at the geometric centroids of the Voronoi cells, denoted $\hat{\mathbf{c}}_i$, $i=1,\ldots,n$. The centroids are not necessarily coincident with the nuclei $\mathbf{c}_i$, $i=1,\ldots,n$. The orientation field $\boldsymbol{\Psi}(\mathbf{x})$, $\mathbf{x}\in D$ is completely defined by the sample grain geometry and the random vector $\hat{\boldsymbol{\Psi}}$ which has components defined by

$$\hat{\boldsymbol{\Psi}}_i = \Psi_1(\hat{\mathbf{c}}_i) \tag{11}$$

$$\hat{\boldsymbol{\Psi}}_{n+i} = \Psi_2(\hat{\mathbf{c}}_i) \tag{12}$$

$$\hat{\boldsymbol{\Psi}}_{2n+i} = \Psi_3(\hat{\mathbf{c}}_i), \quad i=1,\ldots,n \tag{13}$$

The correlation structure of this random vector is such that it has a scaled covariance matrix

$$\hat{\boldsymbol{\rho}}=\begin{bmatrix}\hat{\boldsymbol{\rho}}_{11} & \hat{\boldsymbol{\rho}}_{12} & \hat{\boldsymbol{\rho}}_{13}\\ \hat{\boldsymbol{\rho}}_{21} & \hat{\boldsymbol{\rho}}_{22} & \hat{\boldsymbol{\rho}}_{23}\\ \hat{\boldsymbol{\rho}}_{31} & \hat{\boldsymbol{\rho}}_{32} & \hat{\boldsymbol{\rho}}_{33}\end{bmatrix} \tag{14}$$

Defining $d_{ij}=\|\hat{\mathbf{c}}_i-\hat{\mathbf{c}}_j\|$ to be the distance between the geometric centroids of $p_i$ and $p_j$, the submatrices $\hat{\boldsymbol{\rho}}_{ij}$ have components (see Table 2)

$$\hat{\rho}_{ij,pq}=\rho_{ij}(d_{pq}) \tag{15}$$

The random vector $\hat{\boldsymbol{\Psi}}$ is modeled as a translation vector whose Gaussian image $\hat{\mathbf{V}}$ has scaled covariance matrix $\hat{\boldsymbol{\xi}}$ given by Eq. (10).

Given this definition of the random vector $\hat{\boldsymbol{\Psi}}$ the procedure for generating a realization of the orientation field is (conditional upon a tessellation with grains $p_i$, $i=1,\ldots,n$)

1. Calculate the geometric centroids $\{\hat{\mathbf{c}}_i\}$ of the grains;
2. Calculate the grain separation distances $\{d_{ij}\}$;
3. Populate the scaled covariance matrix $\hat{\boldsymbol{\xi}}$ of the Gaussian image $\hat{\mathbf{V}}$ of $\hat{\boldsymbol{\Psi}}$;
4. Generate a realization of $\hat{\mathbf{V}}$ by $\hat{\mathbf{V}}=\beta\hat{\mathbf{Z}}$ where $\boldsymbol{\beta}$ is the Cholesky decomposition of $\hat{\boldsymbol{\xi}}$ and $\hat{\mathbf{Z}}$ is a Gaussian random vector with components that are independent identically distributed with mean zero and unit variance; and
5. Transform $\hat{\mathbf{V}}$ into $\hat{\boldsymbol{\Psi}}$ by

$$\hat{\boldsymbol{\Psi}}_i=g_j(\hat{V}_i)\begin{cases} j=1, & 1\leqslant i\leqslant n\\ j=2, & n+1\leqslant i\leqslant 2n\\ j=3, & 2n+1\leqslant i\leqslant 3n\end{cases} \tag{16}$$

The realization $\boldsymbol{\psi}(\mathbf{x})$, $\mathbf{x}\in D$, of the orientation field is completely defined, and is given by

$$\boldsymbol{\psi}(\mathbf{x})=\begin{bmatrix}\hat{\psi}_i\\ \hat{\psi}_{n+i}\\ \hat{\psi}_{2n+i}\end{bmatrix}, \quad \mathbf{x}\in p_i \tag{17}$$

## Intergranular Fracture

The probabilistic model developed for the microstructure and material properties of polycrystalline materials is not useful in an engineering context if it cannot be used to aid in the solution of important problems in probabilistic micromechanics. One such problem is the determination of the propagation paths and rates of microstructurally small cracks subject to possibly uncertain external actions. The complexity of this problem places its detailed solution beyond the scope of this paper. A simplified version of the problem is, however, addressed to indicate the possible application of the probabilistic polycrystal model. It is recognized that the assumptions made detract from the physical realism of the analysis, yet, the solution does demonstrate the types of results which can be obtained using simulation based on the probabilistic polycrystal model.

Realizations of the random polycrystalline microstructure, generated using the procedure described above, are now used in an investigation of uncertainty in the trajectory of intergranular microcracks. The problem analyzed is shown in Fig. 11, namely a polycrystal subject to uniaxial tension with an initial edge crack along one of the grain boundaries.

By limiting the crack to an intergranular trajectory the number of possible crack trajectories is reduced from infinite to some finite, tractable number. A key result of the limitation to intergranular cracks is that only the relative resistance to fracture of the grain boundaries must be known, and not the resistance to fracture of the grain boundaries relative to the intragranular material. Several general assumptions are made regarding the behavior of the crack, namely:

- The crack propagates only along the grain boundaries, that is, it remains intergranular;
- The crack tip always proceeds in the direction of positive $x_1$;
- The crack does not branch; and
- Propagation continues until the polycrystal is severed.

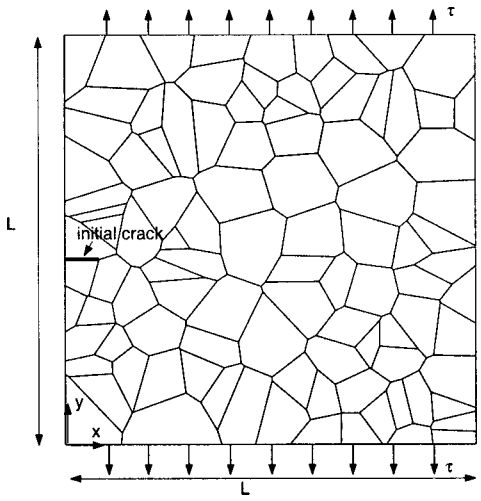


**Fig. 11.** Schematic illustration of example crack propagation problem. A polycrystal subject to uniaxial tension.

### Crack Path Determination

Since the crack is restricted to the grain boundaries, the problem of determining the trajectory is reduced to that shown in Fig. 12; determination of which of two grain boundaries to proceed along when the crack tip encounters a grain boundary junction, or triple point. In the figure, the crack tip is at the junction of the grain boundaries separating grains $p_1$, $p_2$, and $p_3$. These grains have orientations $\boldsymbol{\psi}_i$, $i=1,2,3$, where the underscore in the figure indicates a vector quantity. The grain boundary between grains $p_i$ and $p_j$ is denoted by $b_{ij}$ and has associated with it a misorientation angle $\theta_{ij}$ which is the angle part of the axis/angle representation of the misorientation between $\boldsymbol{\psi}_i$ and $\boldsymbol{\psi}_j$. The dashed line, labeled homogeneous trajectory, indicates the trajectory along which the crack would propagate were it in a homogeneous continuum subject to the remote uniaxial stress $\sigma$. The angle between

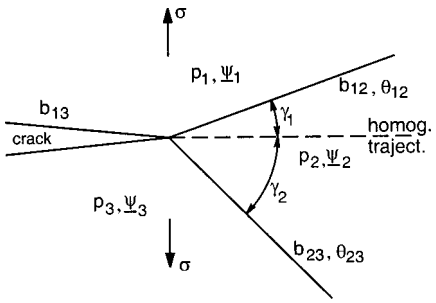


**Fig. 12.** As an intergranular crack approaches a grain boundary junction (triple point), the crack must propagate along one of the candidate grain boundaries

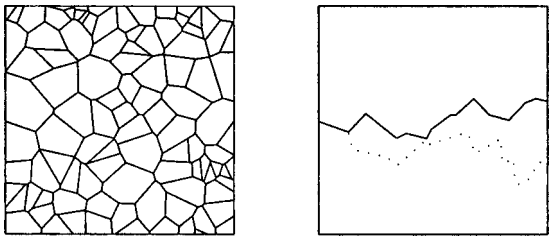

**Fig. 13.** Single realization of intergranular crack growth using both the maximum misorientation and minimum deviation criteria. The solid line corresponds to the minimum deviation criterion and the dashed line to the maximum misorientation criterion.

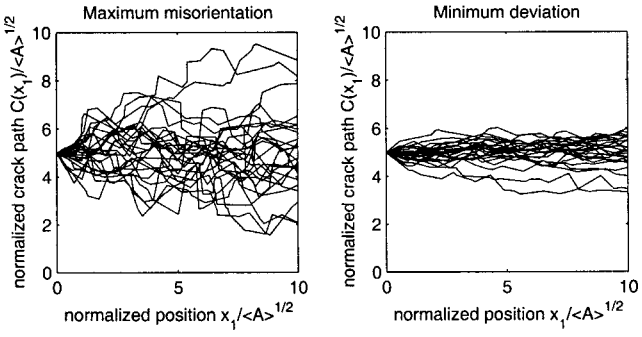


**Fig. 14.** Monte Carlo simulation of intergranular crack growth using both the maximum misorientation and minimum deviation criteria

the homogeneous trajectory and $b_{12}$ is $\gamma_1$ and $\gamma_2$ is the angle between the homogeneous trajectory and $b_{23}$.

While the grain boundary along which propagation occurs can be determined by energy considerations coupled with the principles of linear elastic fracture mechanics (Arwade et al. 1998), the application of such a method requires extremely time consuming finite element analysis and Monte Carlo simulation. As yet, an insufficient number of simulations have been made to allow any conclusions to be drawn regarding the propagation of uncertainty through the system.

Here, two mechanically simplified criteria are used to determine the crack propagation direction at grain boundary junctions. In the first, called the maximum misorientation criterion, the crack is assumed to propagate along the grain boundary which has the larger angle of misorientation, for example, along $b_{23}$ in Fig. 12 if $\theta_{23}>\theta_{12}$. In the second, the minimum deviation criterion, the crack propagates along the grain boundary which lies closest to the homogeneous trajectory. That is, the grain boundary for which the angle $\gamma$ is minimized, which, in Fig. 12 is $b_{12}$ since $\gamma_1<\gamma_2$. These two criteria correspond, respectively, to the cases in which randomness in the crack trajectory is determined by randomness in the material properties or the grain geometry. The maximum misorientation criterion is motivated by the observation that grain boundaries with a high misorientation tend to have lower fracture toughness (Kurishita et al. 1985; Li and Zhang 1995). The minimum deviation criterion is based on the intuition that, for an edge crack under uniaxial tension, the energy release per unit crack extension is greater the closer to perpendicular to the applied stress is the angle of propagation.

These two criteria are chosen in the belief that they represent extremes of the possible fracture behavior; the propagation depending either entirely upon the local material properties (maximum misorientation), or the local grain boundary geometry (minimum deviation). The physical reality likely is a combination of these two effects. As a preliminary attempt to address these intermediate cases, a mixed criterion is introduced. Define the quantity

$$B=W\frac{\theta}{\theta_{\max}}+(1-W)\frac{\gamma_{\max}-\gamma}{\gamma_{\max}} \tag{18}$$

where $\theta_{\max}\approx 62°$ as given by the Mackenzie distribution (Randle 1993), $\gamma_{\max}=90°$ since the crack must always propagate forward, and $W$ is a weight factor. When $W=1$ the maximum misorientation criterion is obtained, and when $W=0$ the minimum deviation criterion is obtained if the crack is assumed to propagate in the direction of greater $B$.

### *Monte Carlo Simulation*

To investigate the propagation of uncertainty in the material microstructure to uncertainty in intergranular crack trajectories Monte Carlo simulation is performed on the problem described above (see Fig. 11). Independent microstructural realizations are generated with the domain of the polycrystal being $D=[0,L]^2$. The crack is assumed to initiate at the grain boundary which intersects $x_1=0$ with $x_2$ coordinate closest to $x_2=L/2$, and the crack tip is advanced using either the minimum deviation or maximum misorientation criterion until the crack tip encounters $x_1=L$. The Monte Carlo simulation provides independent realizations of the random crack paths, denoted by $C(x_1)$. Fig. 13 shows the crack paths determined for a sample microstructure using the two criteria, illustrating the significantly different crack paths obtained by the two methods.

Fig. 14 shows 25 crack path realizations for each criterion. The domain of the samples, with $L=500\,\mu$m, is $D=[0,500]^2\,\mu$m with an average of 100 grains. Two adjustments are made to the crack paths as presented in Fig. 13: the crack paths are normalized using $\tilde{x}_1=x_1/\sqrt{\bar{A}}$ and $\tilde{C}(x_1)=C(x_1)/\sqrt{\bar{A}}$, where $\bar{A}$ is the average grain area, and the initial crack path is shifted so that $C(0)/\sqrt{\bar{A}}=5$. The normalization is applied so that statistics of the crack paths can be computed nondimensionally and to neglect uncertainty in the initiation site of the crack. The side by side comparison of crack paths obtained by the two different criteria indicate that the minimum deviation criterion results in crack paths much closer to the homogeneous trajectory than those obtained by use of the maximum misorientation criterion.

This observation is confirmed by the statistics shown in Fig. 15. The variance of $\tilde{C}(\tilde{x}_1)$ is linear in $\tilde{x}_1$. The growth rates of the

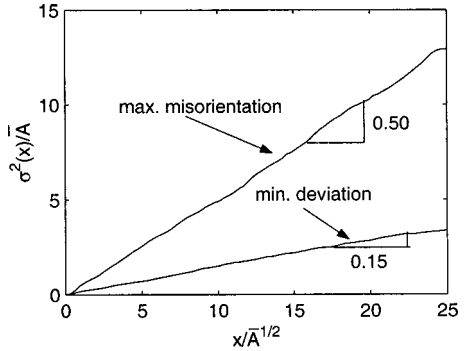


**Fig. 15.** Growth of variance of the crack trajectories

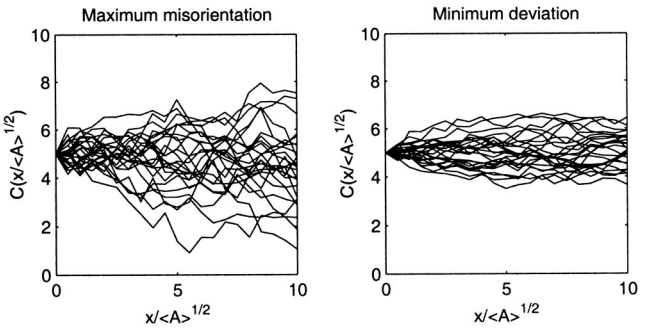


**Fig. 16.** Realizations of crack trajectories generated from scaled Brownian motion model for intergranular cracks

variance are 0.50 and 0.15 with respect to $\tilde{x}_1$ for the maximum misorientation and minimum deviation criteria, respectively.

Some example calculations with the mixed criterion yield some interesting preliminary results. When $W=0.75$, the crack path has a variance growth rate of 0.35, when $W=0.5$ the variance growth rate is 0.21, and when $W=0.25$ the variance growth rate is 0.17. These variance growth rates, corresponding to intermediate values of the criterion weight, demonstrate the nonlinear sensitivity of the variance growth rate to the weight, and also that the minimum deviation criterion appears to dominate for weights close to 1. It is in this regime of intermediate weights that the true behavior of intergranular cracks is expected to be found. Through the use of higher fidelity, but more time consuming mechanical models, future investigation will attempt to further explain the behavior of intergranular cracks in this intermediate regime.

### *Probabilistic Model*

The random nature of the crack paths generated by Monte Carlo simulation, coupled with the observed linear variation of the crack path variance suggests that a scaled Brownian motion may be an appropriate model for intergranular crack trajectories. Let the normalized crack be a random process defined by

$$\tilde{C}(\tilde{x}_1)=\sigma B(\tilde{x}_1) \tag{19}$$

where $B(\tilde{x}_1)$ is a standard normal Brownian motion process, that is, a Gaussian process with stationary independent increments such that $B(u+h)-B(u)$, $h>0$ is $N(0,h)$. The process $\tilde{C}(\tilde{x}_1)$ has zero mean and variance $\mathrm{var}[\tilde{C}(\tilde{x}_1)]=\sigma^2\tilde{x}_1$ if $\mathrm{var}[\tilde{C}(0)]=0$. The parameter $\sigma$ is determined to be $\sqrt{0.50}$ and $\sqrt{0.15}$ for the cases of cracks whose trajectory is determined by the maximum misorientation and minimum deviation criteria, respectively.

To generate realizations of intergranular crack paths a step size $\Delta\tilde{x}_1$ is selected which is equal to 1. An initial condition $\tilde{C}(0)$ is chosen and the crack trajectory is generated by the forward difference equation

$$\tilde{C}(\tilde{x}_{1,i+1})=\tilde{C}(\tilde{x}_{1,i})+(\sigma\sqrt{\Delta\tilde{x}_1})A_i \tag{20}$$

where $\{A_i\}$ are independent standard normal Gaussian random variables. Samples of this process are shown in Fig. 16 for both values of the calibration parameter. The sample trajectories bear a qualitative resemblance to the simulated trajectories of Fig. 14 and match the linear growth of variance. The process can then be rescaled to actual units by $C(x)=\tilde{C}(x/\sqrt{A})\sqrt{A}$. This simulation method can as well be applied to generate crack trajectories corresponding to the mixed propagation criterion introduced earlier. It entails simply finding the value of the variance growth rate for the desired value of $W$, and inserting this value into Eq. (20).

This example illustrates the possibility of using Monte Carlo simulation of microstructural evolution as a means of generating statistics on microstructural features such as crack trajectories. If sufficient confidence can be placed in the mechanics of the models used in the Monte Carlo simulation then direct probabilistic modeling of the evolved microstructures may be possible, allowing generation of sample microstructures at the desired stage of evolution. While the mechanics of the crack propagation models presented here are too simplified to offer such a claim to physical reality, the example serves to illustrate the method and the potential usefulness of the described probabilistic model of polycrystalline microstructures.

## Conclusions

A framework for the numerical simulation of polycrystalline materials is described. The grain geometry is modeled, in two dimensions, by a Poisson–Voronoi tessellation in which the nucleation points of the grains are represented by a Poisson point field and the grains themselves are represented by the cells of a Voronoi tessellation constructed on the nuclei. This model is capable of reproducing grain structures which are isotropic and have stationary average grain size. The model presented is calibrated to experimental measurements in terms of the average grain size, which is related to the intensity of the Poisson point field.

The crystallographic orientation is modeled as a vector random field which is calibrated in marginal distributions and second moment properties. Samples of the orientation field are generated by a memoryless transformation of a Gaussian random field called a translation field. These samples statistically match the experimental data in marginal distribution and second moment properties.

An example application is presented in which realizations of the polycrystalline microstructure are analyzed for fracture subject to uniaxial tension. The trajectory of an intergranular crack through the sample polycrystal is calculated by one of two criteria. The crack is assumed to propagate either along the grain boundary with the largest misorientation—the weaker grain boundary—or the grain boundary which is closest to the trajectory the crack would take in a homogeneous continuum. The inclusion of material effects through the misorientation increases the variability of the crack trajectories. Preliminary investigation of a mixed propagation criterion indicates that the behavior in the mixed regime is nonlinear and complex. Further study is necessary in this regime to achieve physically realistic results.

Using Monte Carlo simulation of the intergranular cracks the crack trajectories were found to exhibit the linear increase of variance which is typical of a Brownian motion process. A scaled Brownian motion was shown to be a qualitatively good model for intergranular cracks with the scaling parameter dependent upon the amount of material dependence. This model can be used to efficiently generate realizations of microcracks which statistically match the cracks generated by Monte Carlo simulation. The example has demonstrated the possibility of using numerical simulation to calibrate probabilistic models for materials at evolved states.

## Notation

*The following symbols are used in this paper:*

$\bar{A}$ = average grain area;

$A$ = grain area;
$B$ = network of grain boundaries;
$b_{ij}$ = grain boundary between $p_i$ and $p_j$;
$\hat{C}(\cdot)$ = normalized crack trajectory;
$C(\cdot)$ = crack trajectory;
$\mathbf{c}$ = covariance function of $\mathbf{\Psi}$;
$\hat{\mathbf{c}}_i$ = grain centroids;
$\mathbf{c}_i$ = grain nuclei;
$\hat{c}_{ij}$ = estimates of covariance functions;
$c_{ij}$ = covariance functions;
$D$ = polycrystal domain;
$d$ = separation distance;
$d_{c,ij}$ = correlation lengths;
$E[\cdot]$ = expectation operator;
$\mathbf{e}_i$ = unit vector;
$F_i(\cdot)$ = cumulative distribution function of $\Psi_i$;
$\mathbf{n}$ = unit vector;
$\hat{p}_{ij}$ = estimates of normalized covariance functions;
$p_i$ = Voronoi polygon;
$\mathbf{V}$ = Gaussian random vector;
$\mathbf{z}_i$ = orientation measurement points;
$\alpha_1, \alpha_2$ = parameters of gamma distribution;
$\boldsymbol{\beta}$ = Cholesky decomposition of $\boldsymbol{\rho}$;
$\Gamma(\cdot)$ = gamma function;
$\gamma_{ij}$ = angle between $b_{ij}$ and homogeneous crack trajectory;
$\gamma_3$ = skewness;
$\gamma_4$ = kurtosis;
$\Delta\hat{x}$ = crack growth increment;
$\theta_{ij}$ = misorientation angle between grains $i$ and $j$ (rad);
$\lambda$ = Poisson point field intensity;
$\mu_i$ = mean of $\Psi_i$;
$\boldsymbol{\xi}$ = scaled covariance of Gaussian image of $\mathbf{\Psi}$;
$\boldsymbol{\rho}$ = scaled covariance function of $\mathbf{\Psi}$;
$\sigma$ = scaling parameter for Brownian motion crack model;
$\sigma_i$ = standard deviation of $\Psi_i$;
$\tau$ = applied stress;
$\Phi(\cdot)$ = standard normal cdf;
$\phi(\cdot,\cdot;\rho)$ = bivariate Gaussian pdf with correlation $\rho$;
$(\phi_1, \Phi, \phi_2)$ = Euler angles, standard notation (rad);
$\mathbf{\Psi}$ = orientation random field; and
$(\psi_1, \psi_2, \psi_3)$ = Euler angles, notation used in current paper (rad).

## References


Adams, B. L. (1993). ''Orientation imaging microscopy: Application to the measurement of grain boundary structure.'' *Mater. Sci. Eng., A,* 166, 59–66.

Adams, B. L., Etinghof, P. I., and Sam, D. D. (1994). ''Coordinate free tensorial representation of n-point correlation functions for microstructure by harmonic polynomials.'' *Proc., 10th Int. Conf. on Textures and Materials*, September 20–24, 1993, Clausthal, Germany, Aedermannsdorf, Switzerland, Trans Tech, 287–294.

Anderson, P. M., and Rice, J. R. (1985). ''Constrained creep cavitation of grain boundary facets.'' *Acta Metall.,* 33, 409–422.

Arwade, S. R., Grigoriu, M., and Ingraffea, A. R. (1998). ''Crack growth in stochastic microstructures.'' *Stochastic Structural Dynamics: Proc., Fourth Int. Conf. on Stochastic Structural Dynamics*, Notre Dame, Ind.

Ballarini, R., Mullen, R. L., and Heuer, A. H. (1999). ''The effects of heterogeneity and anisotropy on the size effect in cracked polycystalline films.'' *Int. J. Fract.,* 95(1), 19–39.

Bunge, H.-J. (1982). *Texture analysis in materials science*, Butterworths, London.

Fradkov, V. E., Kravchenko, A. S., and Schvindlerman, L. S. (1985). ''Experimental investigation of normal grain growth in terms of area and topological class.'' *Scr. Metall.,* 19, 1291–1296.

Gertsman, V. Y. (1997). ''Modelling of intergranular damage propagation.'' *Acta Mater.,* 45, 4107–4116.

Gertsman, V. Y., Janacek, M., and Tangri, K. (1996). ''Grain boundary ensembles in polycrystals.'' *Acta Mater.,* 44, 2869–2889.

Gertsman, V. Y., Zhilyaev, A. P., Pshenichnyuk, A. I., and Valiev, R. Z. (1992). ''Modelling of grain boundary misorientation spectrum in polycrystals with crystallographics texture.'' *Acta Metall. Mater.,* 40, 1433–1441.

Grigoriu, M. (1995). *Applied non-Gaussian processes: Examples, theory, simulation, linear random vibration and MATLAB solutions*, Prentice-Hall, Englewood Cliffs, N.J.

Harlow, D. G., Lu, H.-M., Hittinger, J. A., Delph, T. J., and Wei, R. P. (1996). ''A three-dimensional model for the probabilistic intergranular failure of polycrystalline aggregates.'' *Modell. Simul. Mater. Sci. Eng.,* 4, 261–279.

Kumar, A., and Dawson, P. R. (1998). ''Modeling crystallographic texture evolution with finite elements over neo-Eulerian orientation spaces.'' *Comput. Methods Appl. Mech. Eng.,* 153, 259–302.

Kurishita, H., Kuba, S., Kubo, H., and Yoshinga, H. (1985). ''Misorientation dependance of grain boundary fracture in molybdenum bicrystals with various ⟨110⟩ twist boundaries.'' *Trans. Jpn. Inst. Met.,* 26, 332–240.

Li, G. H., and Zhang, L. D. (1995). ''Relationship between misorientation and bismuth induced embrittlement of [001] tilt boundary in copper bicrystal.'' *Scr. Metall. Mater.,* 32, 1335–1340.

Okazaki, K., and Conrad, H. (1972). ''Grain size distribution in recrystallized alpha-titanium.'' *Trans. Jpn. Inst. Met.,* 13, 198–204.

Randle, V. (1993). *The measurement of grain boundary geometry*, Institute of Physics, Bristol, U.K.

Rhines, F. N., and Patterson, B. R. (1982). ''Effect of the degree of prior cold work on the grain volume distribution and the rate of grain growth of recrystallized aluminum.'' *Metall. Trans. A,* 13A, 985–993.

van der Giessen, E., and Tvergaard, V. (1994a). ''Effect of random variations in microstructure on the development of final creep failure in polycrystalline aggregates.'' *Modell. Simul. Mater. Sci. Eng.,* 2, 721–738.

van der Giessen, E., and Tvergaard, V. (1994b). ''Interaction of cavitating grain boundary facets in creeping polycrystals.'' *Mech. Mater.,* 17, 47–69.

Weyer, S., Fröhlich, A., Riesch-Oppermann, H., Cizelj, L., and Kovac, M. (2002). ''Automatic finite element meshing of planar voronoi tessellations.'' *Eng. Fract. Mech.,* 69, 945–958.

Wilkinson, D. S. (1988). ''The effect of a non uniform void distribution on grain boundary void growth during creep cavitation.'' *Acta Metall.,* 36, 2055–2063.